Dielectric characterization of the charge-ordered nickel oxides: $La_{3/2}Sr_{1/2}NiO_4$ and $La_{5/3}Sr_{1/3}NiO_4$

B. RIVAS-MURIAS[1], J. MIRA[1], A. FONDADO[1], M. A. SEÑARÍS-RODRÍGUEZ[2], J. RIVAS[1]

[1]Dpto. Física Aplicada, Universidad de Santiago de Compostela, E-15782, Santiago de Compostela
[2]Dpto. Química Fundamental, Universidad de A Coruña, E-15071, A Coruña

In this work, we study the dielectric properties of the layered perovskites $La_{3/2}Sr_{1/2}NiO_4$ and $La_{5/3}Sr_{1/3}NiO_4$ in the frequency range 20 Hz- 1 MHz and in the temperature range 110-350 K. For this study, we have synthesized single phase polycrystalline samples by a conventional solid-state reaction. These nickelates show very high values of the dielectric constant at room temperature ($\varepsilon'_r \sim 10^5$), that make them very attractive for potential applications, provided that their rather high losses can be minimized.

The obtained results reveal that even if their dielectric behavior is strongly enhanced by extrinsic polarization effects, there is also a very interesting correlation between their dielectric response and their electronic state.

Keywords: dielectric constant, charge ordering, layered perovskites

Caracterización estructural de los óxidos de níquel con orden de carga: $La_{3/2}Sr_{1/2}NiO_4$ y $La_{5/3}Sr_{1/3}NiO_4$

En este trabajo, se estudian las propiedades dieléctricas de las perovskitas laminares $La_{3/2}Sr_{1/2}NiO_4$ y $La_{5/3}Sr_{1/3}NiO_4$ en el intervalo de frecuencias 20 Hz- 1 MHz y en el intervalo de temperaturas 110-350 K. Para este estudio, se han sintetizado muestras policristalinas y monofásicas mediante el método cerámico. Estos compuestos presentan unos altos valores de la constante dieléctrica a temperatura ambiente ($\varepsilon'_r \sim 10^5$), lo cual los hace muy atractivos para posibles aplicaciones tecnológicas siempre y cuando se puedan reducir sus relativamente altas pérdidas dieléctricas.

Los resultados obtenidos muestran que aunque la respuesta dieléctrica está fuertemente realzada debido a efectos extrínsecos de polarización interfacial, se observa una correlación interesante entre las propiedades dieléctricas y el estado electrónico de los compuestos.

Palabras clave: constante dieléctrica, orden de carga, perovskitas laminares.

1. INTRODUCTION

In the last years there has been an increasing interest in the dielectric properties of perovskites and related structures due to the recent discovery of very high dielectric constants ($\varepsilon'_r \sim 10^4$ at 300 K) first in the $CaCu_3Ti_4O_{12}$ compound (1,2) and later in other compounds such as $AFe_{1/2}B_{1/2}O_3$ (A=Ba, Sr, Ca; B=Nb, Ta, Sb) (3), $Gd_{0.6}Y_{0.4}BaCo_2O_{5.5}$ (4) and $La_{0.5}Sr_{0.5}Ga_{0.6}Ti_{0.4}O_{3-\delta}$ (5).

The origin of these giant dielectric constants is being intensively debated. Many authors, as Lunkenheimer et al. (6,7), Sinclair et al. (8) and Cohen et al. (9) claim that the apparent giant dielectric constants are due to extrinsic effects to the material. They can be explained by Maxwell-Wagner interfacial polarization. This space charge or interfacial polarization is produced by traveling charge carriers.

In our group, we have been investigating the possible link between the electronic process of charge ordering and an increase in the dielectric constant value. The first evidence of this link has been reported by F. Rivadulla et al. (10) in the charge-ordered compound $Pr_{0.67}Ca_{0.33}MnO_3$ (T_{CO}=225 K). Very recently, theoretical studies by Efremov et al. (11) predicted a net polarization of the electric dipole moments in the charge-ordered state.

In this work, we focus on the dielectric behavior of two charge-ordered mixed-oxides: $La_{3/2}Sr_{1/2}NiO_4$ and $La_{5/3}Sr_{1/3}NiO_4$.

These oxides belong to the $La_{2-x}Sr_xNiO_{4\pm\delta}$ series of compounds, that have been the focus of continued studies due to the discovery of superconductivity in the isostructural compounds $La_{2-x}Sr_xCuO_{4\pm\delta}$ (12). Nevertheless, only very recently their dielectric behavior starts to attract attention (13,14).

In the context of charge ordering (CO) both compounds are examples of CO by stripe order. In the nickelates, the stripes are static and take place along the diagonal direction on an tetragonal cell (15,16) and they are characterized by parallel lines of holes that act as charged domain walls separating regions of antiferromagnetically ordered spins. The stripe order is observed for a wide hole concentration region $0.15 \le n_h \le 1/2$ (17,18).

In the $La_{3/2}Sr_{1/2}NiO_4$ compound such a stripe ordering occurs at 180 K (19). The spin ordering occurs at ~80 K and there is a spin reorientation at 57 K (20). At 180 K there is a spontaneous rearrangement of such stripe-type charge order to a checkerboard pattern as seen by neutron diffraction and the checkerboard charge order remains present up to 480 K (19).

In the case of the $La_{5/3}Sr_{1/3}NiO_4$ compound, the sample presents a charge-ordering transition at 240 K which has been observed by electron diffraction (21) and by resistivity, magnetic susceptibility, sound velocity and specific heat (22).

Bol. Soc. Esp. Ceram. V., 45 [3] 169-174 (2006)

169

The spin ordering occurs at ~190 K (23,24) and there is a spin reorientation at 50 K (25).

As these materials are semiconductors, an important extrinsic contribution is to be expected. In order to study the intrinsic and extrinsic contributions (26,27) to the dielectric constant, we have checked the influence of the nature of the contacts used to perform the experiments (sputtered gold and silver contacts).

2. EXPERIMENTAL

The samples were prepared by a conventional solid-state reaction, starting from stoichiometric amounts of dry La_2O_3, $SrCO_3$ and NiO. These materials were thoroughly mixed and grinded together, pressed into pellets and fired at 1373, 1473 and 1573 K with intermediate grindings. The samples were then cooled to room temperature at the rate of 1 K/min.

The samples were characterized by X-ray powder diffraction (XRPD). The XRPD patterns were obtained at room temperature with a Siemens D-5000 diffractometer and Cu (Kα) = 1.5418 Å radiation. The XRPD data were analyzed by the Rietveld method using the Rietica software (28).

The morphology and size of the particles were studied in a scanning electron microscope (SEM), Jeol 6400. Iodometric titrations under an argon flow were carried out to analyze the oxygen content of the samples.

The complex dielectric permittivity was measured with a parallel-plate capacitor coupled to a precision LCR meter Agilent 4284A, capable to measure at frequencies ranging from 20 Hz to 1 MHz and from 110 to 350 K. The capacitor was mounted in an aluminum box refrigerated with liquid nitrogen, and incorporating a mechanism to control the temperature. The samples were prepared to fit in the capacitor and gold was sputtered on their surfaces to ensure good electrical contact with the electrodes.

Additional measurements were performed using different type of contacts (sputtered silver contacts). In addition, to test the optimal performance of the experimental set-up, a commercial $SrTiO_3$ sample was measured and values similar to those reported in the literature (29) were obtained.

Impedance complex plane plots were analyzed using the LEVM program (30).

3. RESULTS AND DISCUSSION

3.1. Structural characterization

The X-ray powder diffraction results indicate that the samples are single phase and show a layered-perovskite structure, the so called K_2NiF_4 structure. In this two-dimensional structure the perovskite blocks, one octahedra thick, are separated from one another by the presence of rock-salt-type (La/Sr-O) layers along the c-axis.

Refinements of the diffraction data indicate that both samples belong to the tetragonal space group I4/mmm with cell parameters a=b=3.8129 (1) Å and c= 12.7416 (2) Å in the sample with x=1/2, and a=b=3.8296 (1) Å and c=12.7123 (2) Å in the case of the sample with x=1/3. These results are in agreement with those reported in the literature (31,32).

According to scanning electron microscopy the obtained polycrystalline materials have an averaged particle diameter

of 2-2.5 μm for x=1/2 and 3-3.5 μm for x =1/3 and show a low degree of sintering (see the corresponding micrographs in figure 1).

As for the iodometric titrations, they indicate that the samples are practically stoichiometric with an oxygen content of 3.99 ±0.01 for x=1/2 and 4.00 ±0.01 for x=1/3.

3.2. Dielectric properties

The relative complex dielectric permittivity $\varepsilon_r(\omega) = \varepsilon'_r(\omega) - i\varepsilon''_r(\omega)$ of the samples as well as their ac conductivity were measured as a function of frequency and temperature.

The results of the real part of the complex relative permittivity, ε'_r (dielectric constant) as a function of frequency are shown in figure 1. As it can be observed in both compounds after an initial decrease at low frequencies, related to diffusion processes, the high dielectric constant keeps a constant value in a wide frequency range, and then decreases in a step-like manner as frequencies get higher. These results are qualitatively similar to those reported in the literature for other compounds such as $CaCu_3Ti_4O_{12}$ (1,2).

The frequency dependence of the imaginary part of the dielectric permittivity, ε''_r of both compounds is displayed in figure 2. As it can be seen, in both cases ε''_r shows rather high values that increase as temperature increases and as
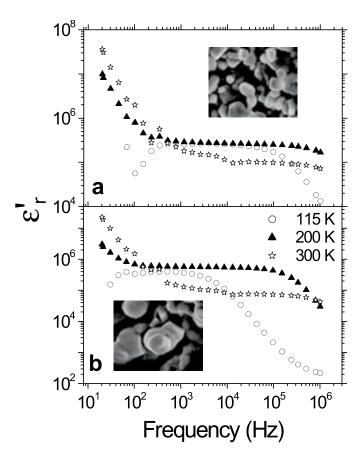

Fig. 1- Real part of the complex relative permittivity, ε'_r versus frequency at selected temperatures, measured with gold contacts, corresponding to $La_{3/2}Sr_{1/2}NiO_4$ (a) and $La_{5/3}Sr_{1/3}NiO_4$ (b). Inset: SEM micrographs of these samples.
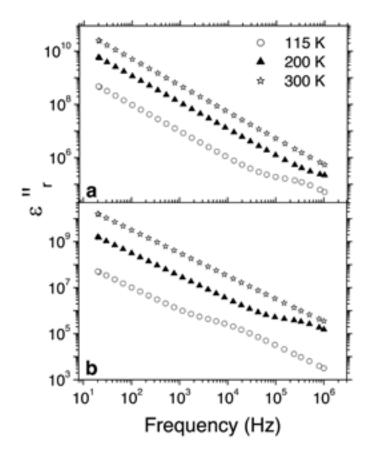
170

Bol. Soc. Esp. Ceram. V., 45 [3] 169-174 (2006)

Fig. 2- Imaginary part of the complex relative permittivity, ε''_r, versus frequency at selected temperatures for La$_{3/2}$Sr$_{1/2}$NiO$_4$ (a) and La$_{5/3}$Sr$_{1/3}$NiO$_4$ (b), measured with gold contacts.

Fig. 3- Frequency dependence of the loss tangent measured at selected temperatures and with gold contacts for the sample La$_{3/2}$Sr$_{1/2}$NiO$_4$ (a) and La$_{5/3}$Sr$_{1/3}$NiO$_4$ (b).

frequency decreases. As a result these samples present rather high losses as it can be observed in figure 3, that shows the frequency dependence of the loss tangent tan δ= $\varepsilon''_r/\varepsilon'_r$ at different temperatures. These high dielectric losses are an important drawback for possible applications, unless they can be minimized.

To try to understand the behavior of these compounds, and taking into account that they are not completely insulating (fig. 4a), we have subtracted from the ε''_r raw data the contribution from free charge carriers (33):

$$\varepsilon''_{r, die}(\omega) = \varepsilon''_r(\omega) - \frac{\sigma_{dc}}{\varepsilon \, \omega}$$ [1]

where $\varepsilon''_{r, die}$ = loss-factor due to the intrinsic dielectric response, σ_{dc}= dc electric conductivity. This dc conductivity υ_{dc} has been obtained from the extrapolation at low frequencies of the conductivity Ó (ω) (see figure 4a).

As an example we show in figure 4b the so-obtained $\varepsilon''_{r, die}$ data as a function of frequency for the x=1/3 sample. It should be noted that there are two maxima: one at low frequencies, that is typical of diffusional processes; and a second one for ν > 10^3 Hz, frequencies at which the very high dielectric constant decreases in a step-like manner. This second maximum (see inset figure 4b) resembles a Debye-like dipolar relaxation process with characteristic relaxation times, τ = 1/ ω, where ω is the characteristic frequency of relaxation. It should be mentioned that there is noticeable increase in the characteristic relaxation times with decreasing temperatures.
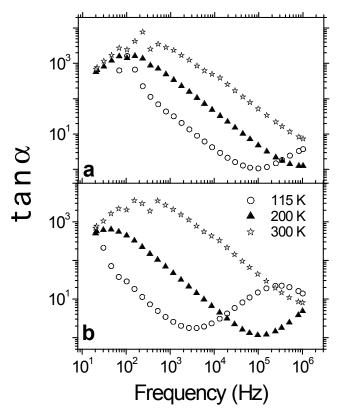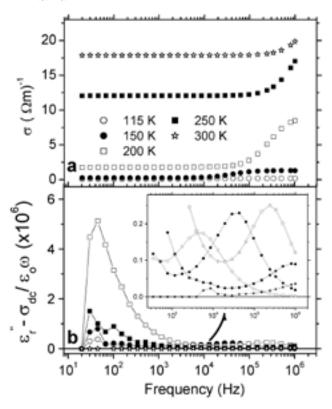

Fig. 4- For the sample with x= 1/3: conductivity versus frequency at different temperatures (a) and frequency dependence of the imaginary part of the complex relative dielectric permittivity after subtraction of the contribution from free charge carriers (b). Inset: enlargement of the high frequency region. Similar results are obtained for the x=1/2 compound.

Bol. Soc. Esp. Ceram. V., 45 [3] 169-174 (2006)

171

On the other hand, if we examine the temperature dependence of ε'_r, we notice the presence of a maximum in the region 160 – 180 K for x=1/2 and 200 – 240 K for x=1/3 (figure 5), just where the formation of stripe charge order is known to take place (19,21).

When we analyze the temperature dependence of σ_{dc}, we observe that in both compounds the conductivity increases monotonically with temperature (fig. 6). Also, very
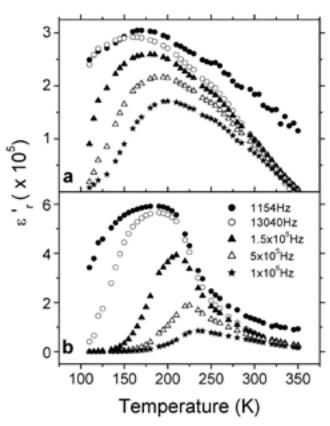

Fig. 5- Dielectric constant, ε'_r, versus temperature at selected frequencies for x=1/2 (a) and x= 1/3 (b), measured with gold contacts.

Fig. 6- Logarithm of σ_{dc} versus the inverse of temperature for the sample with x=1/2 (a) and with x= 1/3 (b).

In view of these data, the dielectric behavior of these materials can be explained on the basis of the extrinsic interfacial Maxwell-Wagner model (26). In this context, the dispersion of ε'_r can be modeled taking into account the interfacial polarization due to the existence of depletion layers near the Au/Ag contacts, and considering the polycrystalline solid as consisting of conducting grains separated by grain boundaries (layers) of lower conductivity (8). In this

interestingly, we find that the thermal activated behavior shows two different activation energies for temperatures above and below those corresponding to the position of the maximum in $\varepsilon'_r(T)$. In the case of the sample with x=1/2, the activation energy is ~75 meV in the high temperature regime (190 <T(K)<320) while it is ~54 meV for 110< T(K) <165 K. In the case of x=1/3, the activation energy is ~45 meV in the high temperature interval (250<T(K)<350) while it is ~65 meV in the region 110-165 K.

To study the influence of extrinsic factors in the dielectric behavior described so far for these samples we have carried out additional measurements using sputtered silver contacts instead of the gold ones. As an example we compare in figure 7 the $\varepsilon'_r(\nu)$ results obtained for the x= 1/2 sample.

As it can be observed in this figure, the dielectric constant values change depending on the nature of the contact, although in both cases they remain very high and keep the same temperature and frequency dependence. These results confirm the influence of extrinsic factors in the observed dielectric response.
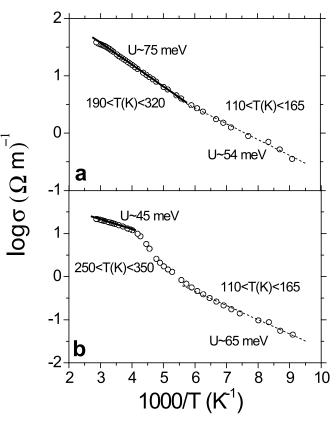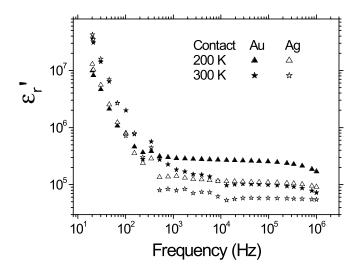

Fig. 7- Plot of ε'_r as a function of frequency for the $La_{3/2}Sr_{1/2}NiO_4$ sample showing the influence of the type of contacts (sputtered gold or silver).

phenomenological model, if we assume that the intrinsic dielectric constant is almost the same in all the sample (in the contacts zone and grain boundaries the conductivity of the material changes, but the dielectric constant should not be too different), then it can be demonstrated (26) that the ε'_r value measured at low frequencies is strongly enhanced by extrinsic contributions that multiply the intrinsic dielectric constant of the compound. The intrinsic ε'_r would directly correspond to ε'_r measured at its optical value ($\omega \rightarrow \infty$), ε'_∞. This optical value is out of the limits of our experimental device whose highest available frequency is 1 MHz.

In order to try to separate the contributions coming from the intrinsic and the extrinsic response we have carried out impedance spectroscopy analysis of the obtained data. Nevertheless the results are not very helpful in this context: what we just obtain in the corresponding impedance complex plane plots for the whole temperature interval is an arc that does not intercept the coordinate origin (fig. 8). This means that, by this technique, in the temperature and frequency range studied we are only able to obtain the contribution coming from extrinsic factors.
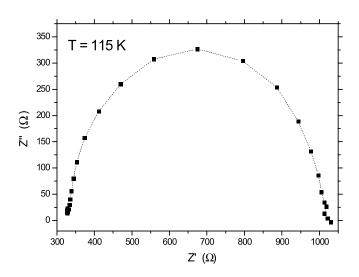

Fig. 8- Example of the Z'' versus Z' diagram found for these samples. The one shown here corresponds to La$_{5/3}$Sr$_{1/3}$NiO$_4$ at 115 K, measured with gold contacts.

In view of this limitation, we have made preliminary measurements of the dielectric constant at higher frequency and by extrapolation we have estimated for these nickelates $\varepsilon'_\infty \approx 40$ at room temperature, a value that is already rather high for these type of compounds (26).

In addition, in the search for any indication about the intrinsic contribution in the here shown results, we find that the variation of ε'_r with temperature is very revealing. As we mentioned before, ε'_r goes through a maximum in the interval $160 - 180$ K for x=1/2 and $200 - 240$ K for x=1/3 (see figure 5). Given that the conductivity of these samples increases monotonically with temperature (fig. 6), so should change the extrinsic contribution to the dielectric constant (26). So why does ε'_r go through a maximum instead of monotonically increase with temperature? Our explanation is that the temperature dependence of ε'_r is shaped by the intrinsic term, that should have a peak in a similar temperature range. And, what is special about those temperatures is that, as mentioned

before, they correspond in both cases to those of formation of stripe charge ordering in these nickelates.

Therefore, there seem to be a link between the electronic state of these materials and their dielectric behavior.

4. CONCLUSIONS

In summary, we have prepared the La$_{3/2}$Sr$_{1/2}$NiO$_4$ and La$_{5/3}$Sr$_{1/3}$NiO$_4$ samples by the ceramic method as single-phase materials.

We have studied the dielectric properties of these two nickelates, finding very high values of the dielectric constant at room temperature ($\varepsilon'_r \sim 10^5$), that make them very attractive for potential applications, provided their rather high losses can be minimized.

Even if these high dielectric constants are strongly enhanced by extrinsic polarization effects, we also find a very interesting correlation between their dielectric response and their electronic state.

This study suggests new possibilities of research on compounds with a high dielectric constant attached to charge-ordering phenomena.

REFERENCES

1. M. A. Subramanian, Dong Li, N. Duan, B. A. Reisner, A. W. Sleight, High dielectric constant in ACu$_3$Ti$_4$O$_{12}$ and ACu$_3$Ti$_3$FeO$_{12}$ phases, J. Solid State Chem. 151, 323-325 (2000).
2. C. C. Homes, T. Vogt, S. M. Shapiro, S. Wakimoto, A. P. Ramirez, Optical response of high-dielectric-constant perovskite-related oxide, Science 293, 673-676 (2001).
3. I. P. Raevski, S. A. Prosandeev, A. S. Bogatin, M. A. Malitskaya, L. Jastrabik, High dielectric permittivity in AFe$_{1/2}$B$_{1/2}$O$_3$ nonferroelectric perovskite ceramics (A=Ba, Sr, Ca; B=Nb, Ta, Sb), J. Appl. Phys. 93, 7, 4130-4136 (2003).
4. V. Bobnar, P. Lunkenheimer, M. Paraskevopoulos, A. Loidl, Separation of grain boundary effects and intrinsic properties in perovskite-like Gd$_{0.6}$Y$_{0.4}$BaCo$_2$O$_{5.5}$ using high-frequency dielectric spectroscopy, Phys. Rev. B 65, 184403-1/5 (2002).
5. E. Iguchi, S. Mochizuki, Electric conduction and dielectric relaxation processes in solid oxide fuel cell electrolyte La$_{0.5}$Sr$_{0.5}$Ga$_{0.6}$Ti$_{0.4}$O$_{3-\delta}$, J. Appl. Phys. 96, 7, 3889-3895 (2004).
6. P. Lunkenheimer, V. Bobnar, A. V. Pronin, A. I. Ritus, A. A. Volkov, A. Loidl, Origin of apparent colossal dielectric constants, Phys. Rev. B 66, 052105-1/4 (2002).
7. P. Lunkenheimer, R. Fichtl, S. G. Ebbinghaus, A. Loidl, Nonintrinsic origin of the colossal dielectric constants in CaCu$_3$Ti$_4$O$_{12}$, Phys. Rev. B 70, 172102-1/4 (2004).
8. D. C. Sinclair, T. B. Adams, F. D. Morrison, A. R. West, CaCu$_3$Ti$_4$O$_{12}$: One-step internal barrier layer capacitor, Appl. Phys. Lett. 80, 12, 2153-2155 (2002).
9. M. H. Cohen, J. B. Neaton, L. He, D. Vanderbilt, Extrinsic models for the dielectric response of CaCu$_3$Ti$_4$O$_{12}$, J. Appl. Phys. 94, 5, 3299-3306 (2003).
10. F. Rivadulla, M. A. López Quintela, L. E. Hueso, C. Jardón, A. Fondado, J. Rivas, M. T. Causa, R. D. Sánchez, Strong ferro-antiferromagnetic competition and charge ordering in Pr$_{0.67}$Ca$_{0.33}$MnO$_3$, Solid State Commun. 110, 179-183 (1999).
11. D. V. Efremov, J. Van den Brink, D. I. Khomskii, Bond-versus site-centred ordering and possible ferroelectricity in manganites, Nature Mater. 3, 853-856 (2004).
12. H. Takagi, B. Batlogg, H. L. Kao, J. Kwo, R. J. Cava, J. J. Krajewski, and W. F. Peck, Jr., Systematic evolution of temperature-dependent resistivity in La$_{2-x}$Sr$_x$CuO$_4$, Phys. Rev. Lett. 69, 20, 2975-2978 (1992).

Bol. Soc. Esp. Ceram. V., 45 [3] 169-174 (2006)

173

13. J. Rivas, B. Rivas-Murias, A. Fondado, J. Mira, M. A. Señarís-Rodríguez, Dielectric response of the charge-ordered two-dimensional nickelate $La_{1.5}Sr_{0.5}NiO_4$, Appl. Phys. Lett. 85, 25, 6224-6226 (2004).

14. T. Park, Z. Nussinov, K. R. A. Hazzard, V. A. Sidorov, A. V. Balatsky, J. L. Sarrao, S.-W. Cheong, M. F. Hundley, J.-S. Lee, Q. X. Jia, J. D. Thompson, Novel dielectric anomaly in the hole-doped $La_2Cu_{1-x}Li_xO_4$ and $La_{2-x}Sr_xNiO_4$ insulators: Signature of an electronic glassy state, Phys. Rev. Lett. 94, 1, 017002-1/4 (2005).

15. J. M. Traquada, D. J. Buttrey, V. Sachan, J. E. Lorenzo, Simultaneous ordering of holes and spins in $La_2NiO_{4.125}$, Phys. Rev. Lett. 73, 7, 1003-1006 (1994).

16. T. Hotta, E. Dagotto, Orbital ordering, new phases, and stripe formation in doped layered nickelates, Phys. Rev. Lett. 92, 7, 227201-1/4 (2004).

17. J. M. Traquada, D. J. Buttrey, V. Sachan, Incommensurate stripe order in $La_{2-x}Sr_xNiO_4$ with x=0.225, Phys. Rev. B 54, 12318-12323 (1996).

18. H. Yoshizawa, T. Kakeshita, R. Kajimoto, T. Tanabe, T. Katsufuji, Y. Tokura, Stripe order at low temperatures in $La_{2-x}Sr_xNiO_4$ with $0.289 \leq x \leq 0.5$, Phys. Rev. B 61, R854-R857 (2000).

19. R. Kajimoto, K. Ishizaka, H. Yoshizawa, and Y. Tokura, Spontaneous rearrangement of the checkerboard charge order to stripe order in $La_{1.5}Sr_{0.5}NiO_4$, Phys. Rev. B 67, 014511-1/5 (2003).

20. P. G. Freeman, A. T. Boothroyd, D. Prabhakaran, M. Enderle, C. Niedermayer, Stripe order and magnetic transitions in $La_{2-x}Sr_xNiO_4$, Phys. Rev. B 70, 024413-1/6 (2004).

21. C. H. Chen, S.-W. Cheong and A. S. Cooper, Charge modulations in $La_{2-x}Sr_xNiO_{4+y}$: Ordering of polarons, Phys. Rev. Lett. 71, 15, 2461-2464 (1993).

22. S.-W. Cheong, H. Y. Hwang, C. H. Chen, B. Batlogg, L. W. Rupp, Jr., and S. A. Carter, Charge-ordered states in $(La,Sr)_2NiO_4$ for hole concentrations $n_h=1/3$ and $1/2$, Phys. Rev. B 49, 7088-7091 (1994).

23. S.-H. Lee, S.-W. Cheong, Melting of quasi-two-dimensional charge stripes in $La_{5/3}Sr_{1/3}NiO_4$, Phys. Rev. Lett. 79, 13, 2514-2517 (1997).

24. P. D. Hattom, M. E. Ghazi, S. B. Wilkins, P. D. Spencer, D. Mannix, T. d'Almeida, P. Prabhakaran, A. Boothroyd, S.-W. Cheong, X-ray scattering studies of charge stripes in $La_{2-x}Sr_xNiO_4$ (x=0.20-0.33), Physica B 318, 289-294 (2002).

25. S.-H. Lee, S.-W. Cheong, K. Yamada, C. F. Majkrzak, Charge and canted spin order in $La_{2-x}Sr_xNiO_4$ (x=0.275 and 1/3), Phys. Rev. B 63, 060405-1/4 (2001).

26. A. von Hippel, Dielectric and Waves, Boston, London, Ed. Artech House (1995).

27. J. C. Maxwell, A Treatise on Electricity and Magnetism, New York, Dover Publications (1954).

28. C. J. Howard, B. A. Hunter, Rietica: "A computer program for Rietveld analysis of X-ray and neutron powder diffraction patterns" Australian Nuclear Science and Technology Organization Lucas Heights Research Laboratories (1997).

29. H. Takashima, R. Wang, N. Kasai, A. Shoji, Preparation of parallel capacitor of epitaxial $SrTiO_3$ film with a single-crystal-like behavior, Appl. Phys. Lett. 83, 14, 2883-2885 (2003).

30. S. H. Han, M. B. Maple, Z. Fisk, S-W. Cheong, A. S. Cooper, O. Chmaissem, J. D. Sullivan, M. Marezio, Structural aspects of pressure-dependent hole ordering in $La_{1.67}M_{0.33}NiO_4$ (M=Ca, Sr, or Ba), Phys. Rev. B 52, 1347-1351 (1995).

31. G. Wu, J. J. Neumeier, C. D. Ling, D. N. Argyriou, Temperature evolution of the crystal structure of $La_{2-x}Sr_xNiO_4$ (x=1/4 and 1/3) as revealed through neutron powder diffraction, Phys. Rev. B 65, 174113-1/8 (2002).

32. A. K. Jonscher, Dielectric Relaxation in Solids, London, Chelsea Dielectric Press, (1983).

◆ ◆ ◆

174

Bol. Soc. Esp. Ceram. V., 45 [3] 169-174 (2006)